MECSOL 2019 - Proceedings of the 7th International Symposium on Solid Mechanics,
V. Tita, A. Ferreira, M.L. Ribeiro, A. Vieira and A.T. Beck (Editors), ABCM, Sao Carlos, SP, Brazil, April 15th to 17th, 2019

BUCKLING OF AXIALLY-COMPRESSED CYLINDRICAL PANELS WITH CIRCULAR EDGE FRAMES ATTACHED

Eliseu Lucena Neto, Rafael Santana, Francisco Monteiro, Paulo Soares*, Airton Souza Neto, and Paulo Queiroz

Instituto Tecnológico de Aeronáutica, 12228-900, São José dos Campos, SP, Brazil

* Centro de Estudos e Projetos de Engenharia da Aeronáutica, 01552-000, São Paulo, SP, Brazil

Abstract: This work presents an exact solution for the boundary-value problem which describes the linear buckling of axially-compressed cylindrical panels with frames attached to the circular edges. The boundary conditions differ from the classical simply supported ones, often assumed for design purposes, in the sense that the torsion resisted by the frames is also taken into account. The presence of the frames makes the results reported herein of practical interest and valuable as benchmark data.

Keywords: exact solution, cylindrical panel, buckling analysis

INTRODUCTION

Circular cylindrical panels are important structural components in many engineering applications, such as aircraft fuselages, exteriors of rockets, submarine hulls, offshore platforms, and many others. The skin of a fuselage, for instance, can be thought of as an assembly of cylindrical panels supported by frames (circumferential stiffeners) and stringers (longitudinal stiffeners). In typical design, these panels are the structural components to buckle first in order to exploit the structure load capacity efficiently (Kollár and Dulácska, 1984, Buermann et al., 2006). An isolated panel, extracted from a skin portion between adjacent stiffeners, can thus be used as a simple solution domain to estimate the skin buckling.

The classical simply supported conditions, often assumed for design purposes, are represented by the requirement that the radial displacements and the bending moments be zero along the edges of an isolated panel, in addition to the constraint of null tangential displacements and normal in-plane stress resultants associated with the buckling deformation. Unlike the above-mentioned conditions, in this paper the bending moments along the panel circular edges are not made zero but equal to the torsion resisted by the attached frames. This will make these edges to be somewhere between simply supported and clamped. The linearized Donnell's equations, with prebuckling rotations neglected, are chosen to describe the panel buckling behavior (Brush and Almroth, 1975). The frames are supposed to resist torsion in two ways: the first is denoted by Saint-Venant torsion, the second by warping torsion (Wunderlich and Pilkey, 2002). For most practical cases, one contribution may be neglected as compared to the other. Warping torsion is usually negligible in bars with solid or thin-walled closed cross sections. Saint-Venant torsion, on the other hand, may be neglected in thin-walled open cross sections (Kollbrunner and Basler, 1969).

Our exact solution is independent of whether the Saint-Venant torsion or the warping torsion are resisted separately or together, and can be used to judge the relevance of each contribution if desired. Our proposed exact solution, which is based on a Lévy-type procedure (Reddy, 2004), has been motivated by the authors' need of benchmarks to test the accuracy of a fast tool under development to predict the skin buckling of reinforced cylindrical shells. The solution is stated in a suitable detail, identifying all the function spaces where the critical buckling mode should be sought, and used to highlight the effects of the panel aspect ratio, shallowness and frame torsional resistance on the critical load.

FUNDAMENTALS

Figure 1a depicts a circular cylindrical panel of radius R, length a, width b and thickness h, subjected to a uniform distributed axial compressive force p per unit length and referred to a set of orthogonal curvilinear coordinates xyz placed in the panel midsurface. The panel buckling is supposed to be described by the linearized Donnell's equations

$$\nabla^4 u = -\frac{\nu}{R} w_{,xxx} + \frac{1}{R} w_{,xyy} \qquad \nabla^4 v = -\frac{2+\nu}{R} w_{,xxy} - \frac{1}{R} w_{,yyy} \qquad D\nabla^8 w + \frac{Eh}{R^2} w_{,xxxx} + p\nabla^4 w_{,xx} = 0 \qquad (1)$$

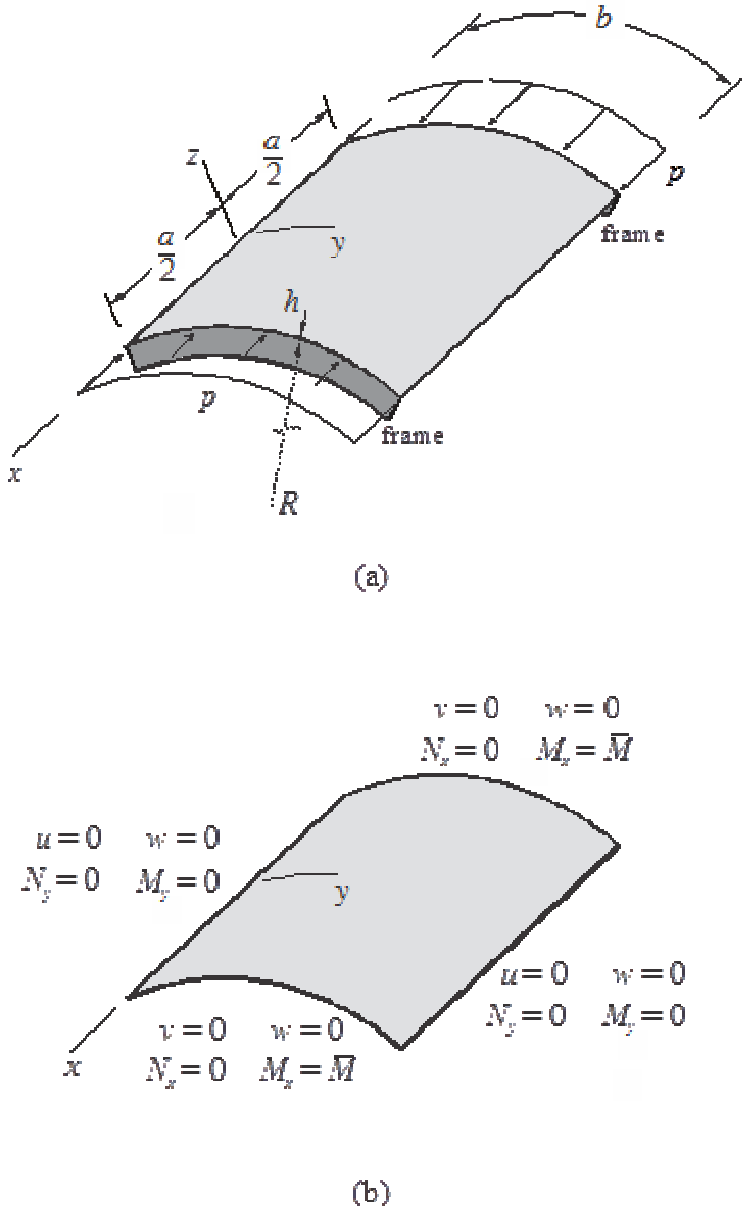

Figure 1 – Cylindrical panel: (a) geometry and loading; (b) boundary conditions

with prebuckling rotations neglected (Brush and Almroth, 1975). The quantities u, v and w are the midsurface displacements in the x, y and z directions, E is the Young's modulus, ν is the Poisson's ratio, $D = Eh^3/12(1-\nu^2)$ defines the panel bending rigidity, $\nabla^8(\,)$ denotes two successive applications of the two-dimensional biharmonic operator $\nabla^4(\,)$ and a comma followed by x (or y) indicates differentiation with respect to x (or y). The boundary conditions (see Fig. 1b) to be applied differ from the classical simply supported ones in the sense that the torsion resisted by the frames attached to the panel circular edges are also taken into account:

$$\begin{array}{llll} N_x = 0 & v = 0 & w = 0 & M_x = \overline{M} \quad \text{at} \quad x = \pm a/2 \\ u = 0 & N_y = 0 & w = 0 & M_y = 0 \quad \text{at} \quad x = 0, b. \end{array} \tag{2}$$

The in-plane forces N_x, N_y and the bending moments M_x, M_y are related to the midsurface displacements by means of

$$\begin{array}{ll} N_x = \dfrac{Eh}{1-\nu^2}\left[u_{,x} + \nu\left(v_{,y} + \dfrac{w}{R}\right)\right] & N_y = \dfrac{Eh}{1-\nu^2}\left(v_{,y} + \dfrac{w}{R} + \nu u_{,x}\right) \\ M_x = -D(w_{,xx} + \nu w_{,yy}) & M_y = -D(w_{,yy} + \nu w_{,xx}) \end{array} \tag{3}$$

and the external moments

$$\overline{M}\left(\pm\frac{a}{2},y\right)=\mp\frac{E_f I_f}{R}\left(u_{,yy}\left(\pm\frac{a}{2},y\right)-\frac{1}{R}w_{,x}\left(\pm\frac{a}{2},y\right)\right)\mp G_f J_f\left(\frac{1}{R}u_{,yy}\left(\pm\frac{a}{2},y\right)+w_{,xyy}\left(\pm\frac{a}{2},y\right)\right)$$
$$\pm E_f\Gamma_f\left(\frac{1}{R}u_{,yyyy}\left(\pm\frac{a}{2},y\right)+w_{,xyyyy}\left(\pm\frac{a}{2},y\right)\right) \tag{4}$$

exerted by the frames on the panel edges $x=\pm a/2$ prevent them from rotating. The frames have torsional and warping constants J_f and Γ_f, area moment of inertia of the cross section about the z axis given by I_f, material with Young's modulus E_f and shear modulus G_f, and are twisted by an amount $-w_{,x}$. The first term in $\overline{M}$ is associated with the frame out-of-plane bending, while the second and third terms are associated with Saint-Venant and warping torsions, respectively.

An exact solution of (1) subjected to (2) can be accomplished most conveniently by introducing the nondimensional coordinates suggested by Nachbar (1962),

$$\xi=\sqrt{\frac{2Eh}{p_{cl}}}\frac{x}{R}\qquad \eta=\sqrt{\frac{2Eh}{p_{cl}}}\frac{y}{R}\qquad p_{cl}=\frac{Eh^2}{R\sqrt{3(1-\nu^2)}}. \tag{5}$$

The classical value p_{cl} identifies the minimum buckling load p that a simply supported panel could ever achieved (Timoshenko and Gere, 1961), according to the adopted linear buckling analysis. Referring to these new coordinates, the system of equations (1) becomes

$$\nabla^4 u=-\nu w_{,\xi\xi\xi}+w_{,\xi\eta\eta}\qquad \nabla^4 v=-(2+\nu)w_{,\xi\xi\eta}-w_{,\eta\eta\eta}\qquad \nabla^8 w+w_{,\xi\xi\xi\xi\xi}+2\rho\nabla^4 w_{,\xi\xi}=0 \tag{6}$$

while the set of boundary conditions (2) reads

$$\begin{array}{lllll} N_\xi=0 & v=0 & w=0 & M_\xi=\overline{M} & \text{at}\quad \xi=\pm\xi_0 \\ u=0 & N_\eta=0 & w=0 & M_\eta=0 & \text{at}\quad \eta=0,\eta_0 \end{array} \tag{7}$$

with

$$\rho=\frac{p}{p_{cl}}\qquad \xi_0=\sqrt{\frac{2Eh}{p_{cl}}}\frac{a}{2R}\qquad \eta_0=\sqrt{\frac{2Eh}{p_{cl}}}\frac{b}{R}. \tag{8}$$

In (6), the operators $\nabla^4(\,)$ and $\nabla^8(\,)$ are written in the new coordinates ξ and η. The quantities

$$u(\xi,\eta)=\sqrt{\frac{2Eh}{p_{cl}}}\frac{u(x,y)}{R}\qquad v(\xi,\eta)=\sqrt{\frac{2Eh}{p_{cl}}}\frac{v(x,y)}{R}\qquad w(\xi,\eta)=\frac{w(x,y)}{R} \tag{9}$$

now represent nondimensional displacement parameters and

$$N_\xi=\frac{Eh}{1-\nu^2}[u_{,\xi}+\nu(v_{,\eta}+w)]\qquad N_\eta=\frac{Eh}{1-\nu^2}(v_{,\eta}+w+\nu u_{,\xi})$$
$$M_\xi=-\frac{D}{R}\frac{2Eh}{p_{cl}}(w_{,\xi\xi}+\nu w_{,\eta\eta})\qquad M_\eta=-\frac{D}{R}\frac{2Eh}{p_{cl}}(w_{,\eta\eta}+\nu w_{,\xi\xi})$$
$$\overline{M}(\pm\xi_0,\eta)=\mp\frac{E_f I_f}{R^2}\sqrt{\frac{2Eh}{p_{cl}}}\left(u_{,\eta\eta}(\pm\xi_0,\eta)-w_{,\xi}(\pm\xi_0,\eta)\right)\mp\frac{G_f J_f}{R^2}\sqrt{\frac{2Eh}{p_{cl}}}\left(u_{,\eta\eta}(\pm\xi_0,\eta)+\frac{2Eh}{p_{cl}}w_{,\xi\eta\eta}(\pm\xi_0,\eta)\right) \tag{10}$$
$$\pm\frac{E_f\Gamma_f}{R^4}\left(\frac{2Eh}{p_{cl}}\right)^{3/2}\left(u_{,\eta\eta\eta\eta}(\pm\xi_0,\eta)+\frac{2Eh}{p_{cl}}w_{,\xi\eta\eta\eta\eta}(\pm\xi_0,\eta)\right).$$

SOLUTION FOR ρ > 1

A general buckling mode satisfying the simply supported boundary conditions on edges $\eta = 0, \eta_0$, can be assumed in the form

$$u(\xi,\eta) = U(\xi)\sin k\eta \qquad v(\xi,\eta) = V(\xi)\cos k\eta \qquad w(\xi,\eta) = W(\xi)\sin k\eta \qquad k = \frac{n\pi R}{b}\sqrt{\frac{p_{cl}}{2Eh}}, \tag{11}$$

with the integer n standing for the number of half-waves in the circumferential direction. The functions $U(\xi)$, $V(\xi)$ and $W(\xi)$ must be obtained so that the mode fulfills the conditions required by the supports at $\xi = \pm\xi_0$ and satisfies (6). After substitution of (11), the boundary conditions (7) on edges $\xi = \pm\xi_0$ hold for every $0 < \eta < \eta_0$ if

$$\begin{gathered} U_{,\xi}(\pm\xi_0) = 0 \qquad V(\pm\xi_0) = 0 \qquad W(\pm\xi_0) = 0 \\ \frac{D}{R}W_{,\xi\xi\xi}(\pm\xi_0) \pm \sqrt{\frac{p_{cl}}{2Eh}}\left(\frac{E_f I_f}{R^2} + \frac{n^2\pi^2}{b^2}G_f J_f + \frac{n^4\pi^4}{b^4}E_f\Gamma_f\right)W_{,\xi}(\pm\xi_0) \\ \pm\frac{n^2\pi^2}{b^2}\left(\frac{p_{cl}}{2Eh}\right)^{3/2}\left(E_f I_f + G_f J_f + \frac{n^2\pi^2}{b^2}E_f\Gamma_f\right)U(\pm\xi_0) = 0. \end{gathered} \tag{12}$$

On the other hand, the equation obtained after substitution of $w(\xi,\eta)$ into the third of equations (6) holds for every point (ξ,η) of the domain for nontrivial w (i.e., $W \neq 0$) if

$$\frac{d^8W}{d\xi^8} - 2(2k^2-\rho)\frac{d^6W}{d\xi^6} + (6k^4 - 4\rho k^2 + 1)\frac{d^4W}{d\xi^4} - 2k^4(2k^2-\rho)\frac{d^2W}{d\xi^2} + k^8W = 0. \tag{13}$$

Particular solutions of this homogeneous linear differential equation are in the form $e^{s\xi}$, where s denotes a root of the algebraic equation

$$s^8 - 2(2k^2-\rho)s^6 + (6k^4 - 4\rho k^2 + 1)s^4 - 2k^4(2k^2-\rho)s^2 + k^8 = 0. \tag{14}$$

The roots of (14) can be easily found by rewriting the equation as

$$\left(\frac{s^2-k^2}{s}\right)^4 + 2\rho\left(\frac{s^2-k^2}{s}\right)^2 + 1 = 0 \tag{15}$$

from which

$$s = \pm\imath\frac{\sqrt{\lambda_j} + \sqrt{\lambda_j - 4k^2}}{2} \qquad \lambda_1 = \rho - \sqrt{\rho^2-1} \qquad \lambda_2 = \rho + \sqrt{\rho^2-1}. \tag{16}$$

It is clear from physical considerations that the buckling will always take place for $\rho > 1$ due to the attachment of frames to the panel edges $\xi = \pm\xi_0$. In view of this evidence, the parameters $\lambda_2 > \lambda_1 > 0$. The presence of the constant term k^8 $(k > 0)$ in (14) and the property $\lambda_j > 0$ anticipate that zero and real roots do not exist. Depending on the values of λ_j and k, the roots may be grouped according to the five cases in the sequel.

Case I: $0 < k^2 < \lambda_1/4$

All the roots are distinct and purely imaginary:

$$s_1 = -s_5 = \imath\gamma_1 \qquad s_2 = -s_6 = \imath\gamma_2 \qquad s_3 = -s_7 = \imath\gamma_3 \qquad s_4 = -s_8 = \imath\gamma_4 \tag{17}$$

with

$$\left.\begin{matrix}\gamma_1\\ \gamma_2\end{matrix}\right\} = \frac{\sqrt{\lambda_1}+\sqrt{\lambda_1-4k^2}}{2} \qquad \left.\begin{matrix}\gamma_3\\ \gamma_4\end{matrix}\right\} = \frac{\sqrt{\lambda_2}+\sqrt{\lambda_2-4k^2}}{2}. \tag{18}$$

The solution of (13) may then be taken in the form

$$W(\xi) = \sum_{i=1,4}\left(w_{is}\cos\gamma_i\xi + w_{ia}\sin\gamma_i\xi\right) \tag{19}$$

where w_{is}, w_{ia} are arbitrary constants.

Because the yz plane is a symmetry plane for the structure (see Fig. 1a), the buckling modes can be separated into two distinct symmetry classes, which may be readily identified by the shape of $W(\xi)$. The modes may be classified by whether the displacement component w is symmetric or antisymmetric with respect to the yz plane. The displacement components u and v will then also have appropriate symmetries. This separation not only aids in identifying and classifying the buckling mode, but also reduces the eigenvalue problem to two distinct problems with smaller determinants to be evaluated. Using the subscripts "s" and "a" to refer to symmetric and antisymmetric parts, the equation (19) splits into

$$W_s(\xi) = \sum_{i=1,4} w_{is}\cos\gamma_i\xi \qquad W_a(\xi) = \sum_{i=1,4} w_{ia}\sin\gamma_i\xi. \tag{20}$$

From (6), (11) and (20), the functions $U(\xi)$ and $V(\xi)$ may also be split into

$$\begin{aligned} U_s(\xi) &= \sum_{i=1,4} w_{is}u_{is}\sin\gamma_i\xi \qquad U_a(\xi) = \sum_{i=1,4} w_{ia}u_{ia}\cos\gamma_i\xi \\ V_s(\xi) &= \sum_{i=1,4} w_{is}v_{is}\cos\gamma_i\xi \qquad V_a(\xi) = \sum_{i=1,4} w_{ia}v_{ia}\sin\gamma_i\xi. \end{aligned} \tag{21}$$

The quantities u_{is}, u_{ia}, v_{is} and v_{ia} are detailed in Souza Neto (2017).

Introduction of the symmetric (or antisymmetric) displacement components (20) and (21) into Eq. (12) yields the homogeneous system of equations $[K]\{w\} = \{0\}$, where $\{w\}$ collects w_{is} (or w_{ia}) and matrix $[K]$ is given in Souza Neto (2017). Each root ρ of the equation $\det[K] = 0$ represents a buckling load. Similar expressions to (20) and (21) hold for the remaining cases, for which the quantities u_{is}, u_{ia}, v_{is}, v_{ia} and $[K]$ are also given in Souza Neto (2017), and only the displacement components will be then summarized next.

Case II: $k^2 = \lambda_1/4$

As the parameters $\gamma_1 = \gamma_2$ in (18), the roots (17) reduces to

$$s_1 = s_2 = -s_5 = -s_6 = \imath\gamma_1 \qquad s_3 = -s_7 = \imath\gamma_3 \qquad s_4 = -s_8 = \imath\gamma_4. \tag{22}$$

The solutions (20) and (21) must be modified to account for the repeated roots $s_1 = s_2$ and $s_5 = s_6$:

$$\begin{aligned} W_s(\xi) &= \sum_{i=1,4} w_{is}\cos\gamma_i\xi + w_{2s}(\xi\sin\gamma_2\xi - \cos\gamma_2\xi) & W_a(\xi) &= \sum_{i=1,4} w_{ia}\sin\gamma_i\xi + w_{2a}(\xi\cos\gamma_2\xi - \sin\gamma_2\xi) \\ U_s(\xi) &= \sum_{i=1,4} w_{is}u_{is}\sin\gamma_i\xi + w_{2s}\bar{u}_{2s}\xi\cos\gamma_2\xi & U_a(\xi) &= \sum_{i=1,4} w_{ia}u_{ia}\cos\gamma_i\xi + w_{2a}\bar{u}_{2a}\xi\sin\gamma_2\xi \\ V_s(\xi) &= \sum_{i=1,4} w_{is}v_{is}\cos\gamma_i\xi + w_{2s}\bar{v}_{2s}\xi\sin\gamma_2\xi & V_a(\xi) &= \sum_{i=1,4} w_{ia}v_{ia}\sin\gamma_i\xi + w_{2a}\bar{v}_{2a}\xi\cos\gamma_2\xi. \end{aligned} \tag{23}$$

Case III: $\lambda_1/4 < k^2 < \lambda_2/4$

All the roots are distinct. Roots $s_1 = -s_5 = \alpha_1 + \imath\beta_1$, $s_2 = -s_6 = \alpha_1 - \imath\beta_1$ are the complex roots with $\alpha_1 = \sqrt{k^2 - \lambda_1/4}$, $\beta_1 = \sqrt{\lambda_1}/2$, and roots s_3, s_4, s_7, s_8 are the purely imaginary roots identified in Case I. Splitting the solution of (13) into symmetric and antisymmetric parts as before,

$$
\begin{aligned}
W_s(\xi) &= w_{1s}\sinh\alpha_1\xi\sin\beta_1\xi + w_{2s}\cosh\alpha_1\xi\cos\beta_1\xi + \sum_{i=3,4} w_{is}\cos\gamma_i\xi \\
W_a(\xi) &= w_{1a}\sinh\alpha_1\xi\cos\beta_1\xi + w_{2a}\cosh\alpha_1\xi\sin\beta_1\xi + \sum_{i=3,4} w_{ia}\sin\gamma_i\xi \\
U_s(\xi) &= \sum_{i=1,2} w_{is}(u_{is}\sinh\alpha_1\xi\cos\beta_1\xi + \overline{u}_{is}\cosh\alpha_1\xi\sin\beta_1\xi) + \sum_{i=3,4} w_{is}u_{is}\sin\gamma_i\xi \\
U_a(\xi) &= \sum_{i=1,2} w_{ia}(u_{ia}\sinh\alpha_1\xi\sin\beta_1\xi + \overline{u}_{ia}\cosh\alpha_1\xi\cos\beta_1\xi) + \sum_{i=3,4} w_{ia}u_{ia}\cos\gamma_i\xi \\
V_s(\xi) &= \sum_{i=1,2} w_{is}(v_{is}\sinh\alpha_1\xi\sin\beta_1\xi + \overline{v}_{is}\cosh\alpha_1\xi\cos\beta_1\xi) + \sum_{i=3,4} w_{is}v_{is}\cos\gamma_i\xi \\
V_a(\xi) &= \sum_{i=1,2} w_{ia}(v_{ia}\sinh\alpha_1\xi\cos\beta_1\xi + \overline{v}_{ia}\cosh\alpha_1\xi\sin\beta_1\xi) + \sum_{i=3,4} w_{ia}v_{ia}\sin\gamma_i\xi.
\end{aligned}
\tag{24}
$$

Case IV: $k^2 = \lambda_2/4$

Roots s_1, s_2, s_5, s_6 are the complex roots identified in Case III, whereas s_3, s_4, s_7, s_8 reduce to the purely imaginary roots $s_3 = s_4 = -s_7 = -s_8 = \imath\gamma_3$. The solution of (13) in this case is:

$$
\begin{aligned}
W_s(\xi) &= w_{1s}\sinh\alpha_1\xi\sin\beta_1\xi + w_{2s}\cosh\alpha_1\xi\cos\beta_1\xi + w_{3s}\cos\gamma_3\xi + w_{4s}\xi\sin\gamma_3\xi \\
W_a(\xi) &= w_{1a}\sinh\alpha_1\xi\cos\beta_1\xi + w_{2a}\cosh\alpha_1\xi\sin\beta_1\xi + w_{3a}\sin\gamma_3\xi + w_{4a}\xi\cos\gamma_3\xi \\
U_s(\xi) &= \sum_{i=1,2} w_{is}(u_{is}\sinh\alpha_1\xi\cos\beta_1\xi + \overline{u}_{is}\cosh\alpha_1\xi\sin\beta_1\xi) + \sum_{i=3,4} w_{is}u_{is}\sin\gamma_3\xi + w_{4s}\overline{u}_{4s}\xi\cos\gamma_3\xi \\
U_a(\xi) &= \sum_{i=1,2} w_{ia}(u_{ia}\sinh\alpha_1\xi\sin\beta_1\xi + \overline{u}_{ia}\cosh\alpha_1\xi\cos\beta_1\xi) + \sum_{i=3,4} w_{ia}u_{ia}\cos\gamma_3\xi + w_{4a}\overline{u}_{4a}\xi\sin\gamma_3\xi \\
V_s(\xi) &= \sum_{i=1,2} w_{is}(v_{is}\sinh\alpha_1\xi\sin\beta_1\xi + \overline{v}_{is}\cosh\alpha_1\xi\cos\beta_1\xi) + \sum_{i=3,4} w_{is}v_{is}\cos\gamma_i\xi + w_{4s}\overline{v}_{4s}\xi\sin\gamma_3\xi \\
V_a(\xi) &= \sum_{i=1,2} w_{ia}(v_{ia}\sinh\alpha_1\xi\cos\beta_1\xi + \overline{v}_{ia}\cosh\alpha_1\xi\sin\beta_1\xi) + \sum_{i=3,4} w_{ia}v_{ia}\sin\gamma_i\xi + w_{4a}\overline{v}_{4a}\xi\cos\gamma_3\xi.
\end{aligned}
\tag{25}
$$

Case V: $\lambda_2/4 < k^2$

All the roots are distinct and complex: $s_1 = -s_5 = \alpha_1 + \imath\beta_1$, $s_2 = -s_6 = \alpha_1 - \imath\beta_1$, $s_3 = -s_7 = \alpha_2 + \imath\beta_2$, $s_4 = -s_8 = \alpha_2 - \imath\beta_2$ with $\alpha_i = \sqrt{k^2 - \lambda_i/4}$, $\beta_i = \sqrt{\lambda_i}/2$. Now, the solution of (13) is

$$
\begin{aligned}
W_s(\xi) &= \sum_{i=1,2} (w_{(2i-1)s}\sinh\alpha_i\xi\sin\beta_i\xi + w_{(2i)s}\cosh\alpha_i\xi\cos\beta_i\xi) \\
W_a(\xi) &= \sum_{i=1,2} (w_{(2i-1)a}\sinh\alpha_i\xi\cos\beta_i\xi + w_{(2i)a}\cosh\alpha_i\xi\sin\beta_i\xi) \\
U_s(\xi) &= \sum_{i=1,2} [(w_{(2i-1)s}u_{(2i-1)s} + w_{(2i)s}u_{(2i)s})\sinh\alpha_i\xi\cos\beta_i\xi + (w_{(2i-1)s}\overline{u}_{(2i-1)s} + w_{(2i)s}\overline{u}_{(2i)s})\cosh\alpha_i\xi\sin\beta_i\xi] \\
U_a(\xi) &= \sum_{i=1,2} [(w_{(2i-1)a}u_{(2i-1)a} + w_{(2i)a}u_{(2i)a})\sinh\alpha_i\xi\sin\beta_i\xi + (w_{(2i-1)a}\overline{u}_{(2i-1)a} + w_{(2i)a}\overline{u}_{(2i)a})\cosh\alpha_i\xi\cos\beta_i\xi] \\
V_s(\xi) &= \sum_{i=1,2} [(w_{(2i-1)s}v_{(2i-1)s} + w_{(2i)s}v_{(2i)s})\sinh\alpha_i\xi\sin\beta_i\xi + (w_{(2i-1)s}\overline{v}_{(2i-1)s} + w_{(2i)s}\overline{v}_{(2i)s})\cosh\alpha_i\xi\cos\beta_i\xi] \\
V_a(\xi) &= \sum_{i=1,2} [(w_{(2i-1)a}v_{(2i-1)a} + w_{(2i)a}v_{(2i)a})\sinh\alpha_i\xi\cos\beta_i\xi + (w_{(2i-1)a}\overline{v}_{(2i-1)a} + w_{(2i)a}\overline{v}_{(2i)a})\cosh\alpha_i\xi\sin\beta_i\xi].
\end{aligned}
\tag{26}
$$

NUMERICAL RESULTS

The nonlinear eigenvalue problem $[K]\{w\}=\{0\}$ cannot be written in a form to allow the direct use of some standard software package to solve it. The following iteration steps is then employed to identify the smallest root ρ of $\det[K]=0$ for a given n:

1. evaluate k from (11);
2. define the open intervals $I_1=(1+\varepsilon,\alpha-\varepsilon)$, $I_2=(\alpha+\varepsilon,2\alpha-2\varepsilon)$ with $\varepsilon=10^{-6}$ and $\alpha=(16k^4+1)/8k^2$;
3. state the small increment $\Delta I_1=10^{-4}[(\alpha-\varepsilon)-(1+\varepsilon)]$ and $\Delta I_2=10^{-4}(\alpha-\varepsilon)$;
4. if $k<1/4$ then Case I, II or III applies.

Case I: starting from $\rho=1+\varepsilon$ verify the sign of $\det[K]=0$ with K_{ij} given for symmetric and for antisymmetric modes. Increase progressively the value of ρ by increments ΔI_1 until either the determinant sign changes or ρ reaches α. If the determinant sign changes, there is a root in the subinterval $[\rho-\Delta I_1,\rho]$ and go to Step 7. If the value of ρ reaches α, then there is no roots in I_1 and go to Case II.

Case II: setting $\rho=\alpha$, verify if $\det[K]=0$ with K_{ij} given for symmetric and for antisymmetric modes. If yes, save the root and go to Step 8. Otherwise, go to Case III. It has been accepted as null the value $|\det[K]|<10^{-3}\varepsilon$.

Case III: starting from $\rho=\alpha+\varepsilon$, verify the sign of $\det[K]=0$ with K_{ij} given for symmetric and for antisymmetric modes. Increase progressively the value of ρ by increments ΔI_2 until either the determinant sign changes or ρ reaches 2α. If the determinant sign changes, there is a root in the subinterval $[\rho-\Delta I_2,\rho]$ and go to Step 7. If the value of ρ reaches 2α, then there is no roots in I_2 and stop the search for the given n;

5. if $k=1/4$ then only Case III applies. Do the Case III process as described previously;
6. if $k>1/4$ then Case V, IV or III applies.

Case V: starting from $\rho=1+\varepsilon$, verify the sign of $\det[K]=0$ with K_{ij} given for symmetric and for antisymmetric modes. Do the same process as described for Case I. If ρ reaches α, then there is no roots in I_1 and go to Case IV.

Case IV: setting $\rho=\alpha$, verify if $\det[K]=0$ with K_{ij} given for symmetric and for antisymmetric modes. If yes, save the root and go to Step 8. Otherwise, go to Case III.

Case III: do the Case III process as described in Step 4;

7. search for the root in the subinterval using some iterative methods. Herein one has employed the *fzero* function of MATLAB that finds a point where the function changes sign using a combination of bisection, secant, and inverse quadratic interpolation methods. Save the root;
8. retain the smallest root ρ, for the given n, with regard to the symmetric and antisymmetric modes.

The critical value of ρ corresponds to the smallest value identified for $n=1,2,3,\ldots$ It is expected that the Cases II and IV will be rarely activated.

All the analyzed panels have length $a=500$ mm, thickness $h=1$ mm, and material defined by $E=72400$ N/mm^2, $\nu=0.33$. Several values are attributed to the width b, radius R, and also to the frame parameters J_f, Γ_f and I_f. The frame material is given by $E_f=71020$ N/mm^2, $G_f=26700$ N/mm^2. Table 1 summarizes the effect of the aspect ratio b/a and radius-to-thickness ratio R/h on the critical value of ρ for panels under different frame torsional J_f, warping Γ_f and flexural I_f constants. Triples ($J_f\neq 0$, $\Gamma_f\neq 0$, $I_f\neq 0$) identify panels with stringers attached to the circular edges. For such panels, the exact buckling loads presented in Table 1 are practically the same than those predicted by neglecting the frame contribution ($J_f=0$, $\Gamma_f=0$, $I_f=0$), i.e., under the classical simply supported boundary condition assumption.

Table 1 – Effect of the aspect ratio and radius-to-thickness ratio on constants.

(J_f, Γ_f, I_f)	b/a	$R/h = 500$	$R/h = 1000$	$R/h = 1500$
(0,0,0)	0.2	1.00171	1.01779	1.18156
	0.4	1.00152	1.00256	1.00122
	0.6	1.00004	1.00102	1.00004
	0.8	1.00000	1.00012	1.00026
	1.0	1.00018	1.00000	1.00017
	1.2	1.00004	1.00001	1.00004
	1.4	1.00000	1.00001	1.00018
(96,36370,853)	0.2	1.00648	1.02663	1.20793
	0.4	1.00648	1.01776	1.00601
	0.6	1.00447	1.01352	1.00388
	0.8	1.00083	1.00573	1.00384
	1.0	1.00209	1.00607	1.01187
	1.2	1.00334	1.00355	1.00388
	1.4	1.00063	1.00237	1.00103

CONCLUSION

A Lévy-type procedure is adopted to develop, in a suitable detail, an exact solution for buckling of axially-compressed cylindrical panels with frames attached to the circular edges. The linearized Donnell's equations, with prebuckling rotations neglected, are chosen to describe the buckling behavior. Both Saint-Venant and warping torsions resisted by the frames are taken into account. For convenience, rather than a necessity, the solution is restricted to load parameters $\rho > 1$ by anticipating the frame presence. An algorithm to generate numerical results is provided. Sets of exact results for specific panels and frames are tabled with which those from approximated procedures may be directly compared. Attaching frames do not have a noteworthy influence on the buckling load of axially-compressed cylindrical panels when compared to the classical simply supported boundary condition assumption.

REFERENCES

Brush, D.O. and Almroth, B.O., 1975, "Buckling of Bars, Plates, and Shells", McGraw-Hill, New York.

Buermann, P., Rolfes, R., Tessmer, J. and Schagerl, M., 2006, "A Semi-Analytical Model for Local Post-Buckling Analysis of Stringer- and Frame-Stiffened Cylindrical Panels", Thin-Walled Structures, Vol. 44, pp. 102–114.

Kollár, L. and Dulácska E., 1984, "Buckling of Shells for Engineers", Wiley, Chichester.

Kollbrunner, C.F. and Basler, K., 1969, "Torsion in Structures", Springer, Berlin.

Nachbar, W., 1962, "Characteristic Roots for Donnell's Equations with Uniform Axial Prestress", Journal of Applied Mechanics, Vol. 29, pp. 434–435.

Reddy, J.N., 2004, "Mechanics of Laminated Composite Plates and Shells: Theory and Analysis", CRC Press, Boca Raton.

Souza Neto, A.F., 2017, "Exact Solution for Buckling of Axially-Compressed Cylindrical Panels with Frames Attached to the Circular Edges", Trabalho de Graduação, Instituto Tecnológico de Aeronáutica, São Paulo, Brazil.

Timoshenko, S.P. and Gere, J.M., 1961, "Theory of Elastic Stability", 2nd ed., McGraw-Hill, New York.

Wunderlich, W. and Pilkey, W.D., 2002, "Mechanics of Structures: Variational and Computational Methods", 2nd ed., CRC Press, Boca Raton.

RESPONSIBILITY NOTICE

The author(s) is (are) the only responsible for the printed material included in this paper.